PERGAMON

Available online at www.sciencedirect.com

SCIENCE DIRECT®

Continental Shelf Research 23 (2003) 1055–1070

CONTINENTAL SHELF RESEARCH

www.elsevier.com/locate/csr

Optimal estimation of tidal open boundary conditions using predicted tides and adjoint data assimilation technique

Aijun Zhang*, Eugene Wei, Bruce B. Parker

Coast Survey Development Laboratory (CSDL), National Ocean Service/NOAA N/CS13, 1315 East-West Highway, Silver Spring, MD 20910, USA

Received 3 July 2002; received in revised form 13 March 2003; accepted 16 May 2003

Abstract

Lateral tidal open boundary conditions which force tides in the internal region are estimated by an adjoint data assimilation system which assimilates predicted coastal tidal elevations into a two-dimensional Princeton Ocean Model for the East Coast of the United States. Control variables are the harmonic constants (amplitude and phase) of tidal constituents (M_2, S_2, N_2, K_1, O_1) along the open boundary. The cost function is defined by the difference between predicted and model-simulated tidal elevations at coastal tide gauge locations. The limited memory Broyden–Fletcher–Goldfarb–Shanno quasi-Newton method for large-scale optimization is implemented to minimize the cost function. Identical twin experiments are performed to verify the adjoint model and to examine sensitivity of model results to the number and spatial distribution of tide gauge stations. The results from the predicted tidal elevation assimilation experiments show that the simulated tidal elevations forced by the optimal open boundary conditions are more accurate than those forced by the open boundary conditions derived from Schwiderski's global tidal model. For M_2 constituent, the maximum RMS error at tide gauge stations with data assimilation is generally 14 cm and the minimum correlation coefficient is 0.96. For the nine open coastal stations, the RMS errors are less than 5 cm. The results from the experiment in which five tidal constituents are considered together show that the RMS errors at the nine open coastal stations are less than 7 cm, and the correlation coefficients are greater than 0.99.
Published by Elsevier Ltd.

Keywords: Tidal open boundary estimation; Tide Gauge data; Adjoint data assimilation; POM

1. Introduction

Open boundary conditions have critical impacts for a regional tidal model. Solutions in model interior are uniquely determined by the tidal open boundary conditions. Traditionally, tidal open boundary conditions can be obtained from either available observations near the open boundaries (tidal gauge data or satellite data), or from large-scale numerical models such as Schwiderski's global tidal model (Schwiderski, 1980) and the TPX0.3 global tidal model (Egbert et al., 1994). Unfortunately, observations at open waters are often scarce and the global tidal model results are less accurate in shallow waters. Therefore, determination of the open boundary conditions might be a limiting factor in developing a regional tidal simulation.

*Corresponding author. Fax: +1-301-713-4501.
E-mail address: aijun.zhang@noaa.gov (A. Zhang).

0278-4343/03/$ - see front matter Published by Elsevier Ltd.
doi:10.1016/S0278-4343(03)00105-5

Chen and Mellor (1999) determined optimal tidal open boundary for a two-dimensional linear Princeton Ocean Model (POM) by using tide gauge data with a simple least squares scheme. For their method, response functions which, in a practical sense, represented complete information on model solutions for arbitrary open boundary forcing, had to be predetermined empirically. Recently, the adjoint method has been widely applied in parameter estimation by assimilating observations into hydrodynamic models. Bennett and McIntosh (1982) and Bennett (1985) used the adjoint variational method to determine the open boundary conditions in the tidal model and array design by using constructed pseudo-observations. Hall et al. (1982) and Cacuci (1988) used the adjoint method to estimate the sensitivity of model forecasts to changes in boundary conditions and model parameters. Seiler (1993) performed a series of identical twin assimilation experiments using the adjoint method to estimate lateral open boundary values of stream function and relative vorticity for a quasi-geostrophic open-ocean model. Heemink et al. (2002) used adjoint approach for the TRIWAQ three-dimensional shallow water flow system to estimate the harmonic constants in the open boundary conditions, the friction parameter, viscosity parameter and water depth by assimilating tide gauge data as well as altimeter data. They showed that the model results were improved considerably.

The accuracy of altimeter data from satellite in coastal region is still not as good as elevation from tide gauges. Han et al. (2000) showed that the model results of assimilating only tide gauge data were better than that of assimilating both tide gauge data and altimeter data for East China Sea. Along the US east coast, reliable water-level time series at many gauge stations last for several decades, accurate harmonic constants of tidal constituents are therefore available. So this study is concentrated on estimating the optimal tidal open boundary conditions by assimilating only tide gauge data.

The nonlinear two-dimensional POM is used for tidal simulation of the US East Coast. Harmonic constants in the open boundary conditions are used as the control variables. The adjoint model was developed for calculating gradients of the cost function with respect to the control variables. In the US East Coast region the semi-diurnal constituents M_2, S_2 and N_2, and the diurnal constituents K_1 and O_1 account for more than 94% of the tidal potential energy (M_2 constituent is the predominant constituent which itself accounts for more than 80% of the tidal potential energy). Only these five tidal constituents are therefore considered. The adjoint method of obtaining open boundary conditions will be shown to greatly improve the calculated tidal elevations over the open boundary conditions based on Schwiderski's global tidal model.

2. Model description

2.1. Forward model

The two-dimensional POM (Blumberg and Mellor, 1987) including all nonlinear terms was used to simulate tides in the US East Coast region. The same model grid and bathymetry as our previous work (Zhang et al., 2002a) were used. The governing equations are as follows:

$$\frac{\partial h}{\partial t}+\frac{\partial UD}{\partial x}+\frac{\partial VD}{\partial y}=0, \tag{1}$$

$$\frac{\partial UD}{\partial t}+\frac{\partial U^2D}{\partial x}+\frac{\partial UVD}{\partial y}-F_x - (f+\tilde{f})VD+gD\frac{\partial h}{\partial x}-\frac{\tau_b^x}{\rho}=0, \tag{2}$$

$$\frac{\partial VD}{\partial t}+\frac{\partial UVD}{\partial x}+\frac{\partial V^2D}{\partial y}-F_y + (f+\tilde{f})UD+gD\frac{\partial h}{\partial y}-\frac{\tau_b^y}{\rho}=0, \tag{3}$$

where h is elevation of free surface with respect to mean sea level, U and V are vertically averaged velocity components in x and y directions, D and $\tau_b^{x,y}$ are water depth at rest and bottom friction, g is the acceleration due to gravity, f is the Coriolis parameter, ρ is the water density, and the horizontal viscosity and diffusion terms F_x and F_y

are defined as

$$F_x = \frac{\partial}{\partial x}\left[D2A_M \frac{\partial U}{\partial x}\right] + \frac{\partial}{\partial y}\left[DA_M\left(\frac{\partial U}{\partial y} + \frac{\partial V}{\partial x}\right)\right], \quad (4)$$

$$F_y = \frac{\partial}{\partial y}\left[D2A_M \frac{\partial V}{\partial y}\right] + \frac{\partial}{\partial x}\left[DA_M\left(\frac{\partial U}{\partial y} + \frac{\partial V}{\partial x}\right)\right], \quad (5)$$

where A_M, the vertically integrated horizontal eddy viscosity, is defined by the Smagorinsky formulation

$$A_M = C\,\Delta x\,\Delta y \frac{1}{2}|\nabla V + (\nabla V)^T|, \quad (6)$$

where C, a nondimensional parameter, is set to be 0.2 in this study; Δx and Δy are the grid spacings in the x and y directions for each grid cell, and curvature term is

$$\tilde{f} = \frac{V\delta_x(\Delta y)}{\Delta x\,\Delta y} + \frac{U\delta_y(\Delta x)}{\Delta x\,\Delta y}. \quad (7)$$

The quadratic law with bottom friction coefficient, C_b, is used for bottom friction,

$$\tau_b^x = C_b\sqrt{U^2 + V^2}U,$$
$$\tau_b^y = C_b\sqrt{U^2 + V^2}V. \quad (8)$$

At the open boundary (at $j = 1$ in this study), tidal elevations for each tidal constituent are prescribed as

$$h_i(t) = \gamma A_i \cos(\omega t + E - \Theta_i) \quad i = 10, \ldots, 110 \quad (9)$$

in which i is index of the model grid along the open boundary, γ is node factor, A_i is mean amplitude, Θ_i is epoch, ω is angular speed and E is value of equilibrium argument when $t = 0$. Velocities are specified with radiation open boundary formulation.

2.2. Cost function and control variables

The National Ocean Service (NOS) of the US National Oceanic and Atmospheric Administration (NOAA) has been maintaining more than 100 permanent operating water-level stations, called the National Water Level Observation Network (NWLON) (Fig. 1) along the US coast. The accurate harmonic constants of tidal constituents can be obtained from the long-term water-level observations. Therefore, it is feasible to assimilate tidal predicted elevations into a numerical model using the optimal control data assimilation techniques to determine a better tidal open boundary conditions for a regional tidal model, and further to improve coastal tidal simulation. Thus, this study is concentrated on how well the simulated tidal water levels could be improved by assimilating tide gauge water-level data. The cost function is defined as

$$J = \frac{1}{2}\int\int\int_{xyt}(h_m - h_0)^2\,\mathrm{d}x\,\mathrm{d}y\,\mathrm{d}t, \quad (10)$$

where h_m and h_0 are model simulated and predicted tidal elevations, respectively. This cost function measures the distance between model simulated and tidal predicted elevations.

In a time-dependent open domain tidal model, several parameters, such as bottom frictional coefficients, bathymetry, initial conditions and open boundary conditions, could be adjusted to fit the model results to the observations. In the present study, only elevations at the open boundary model grids are used as control variables. This assumes that errors of the simulated elevations are caused by the errors in the elevations along the open boundary that propagated over the interior of the model domain. For each individual tidal constituent, elevation values along the open boundary can be calculated with Eq. (9) if the tidal harmonic constants (amplitude, A and phase, Θ) are determined. In order to reduce the number of control variables, A and Θ of each tidal constituent at a given open boundary grid are taken as a quadratic polynomial (based on the results of Schwiderski's global tidal model at the open boundary),

$$A_i = a_1 f_1 + a_2 f_2 i + a_3 f_3 i^2, \quad (11)$$

$$\Theta_i = a_4 f_4 + a_5 f_5 i + a_6 f_6 i^2, \quad (12)$$

where A_i and Θ_i are amplitude (in meters) and phase (in degrees) of a tidal constituent at open boundary grid, i is index of the model grid along the open boundary, a_1–a_6 are the coefficients of the quadratic polynomials and used as real control variables (six control variables for each tidal constituent). Because of the physical nature of these control variables (different unit and magnitude), the parameters are therefore scaled with the

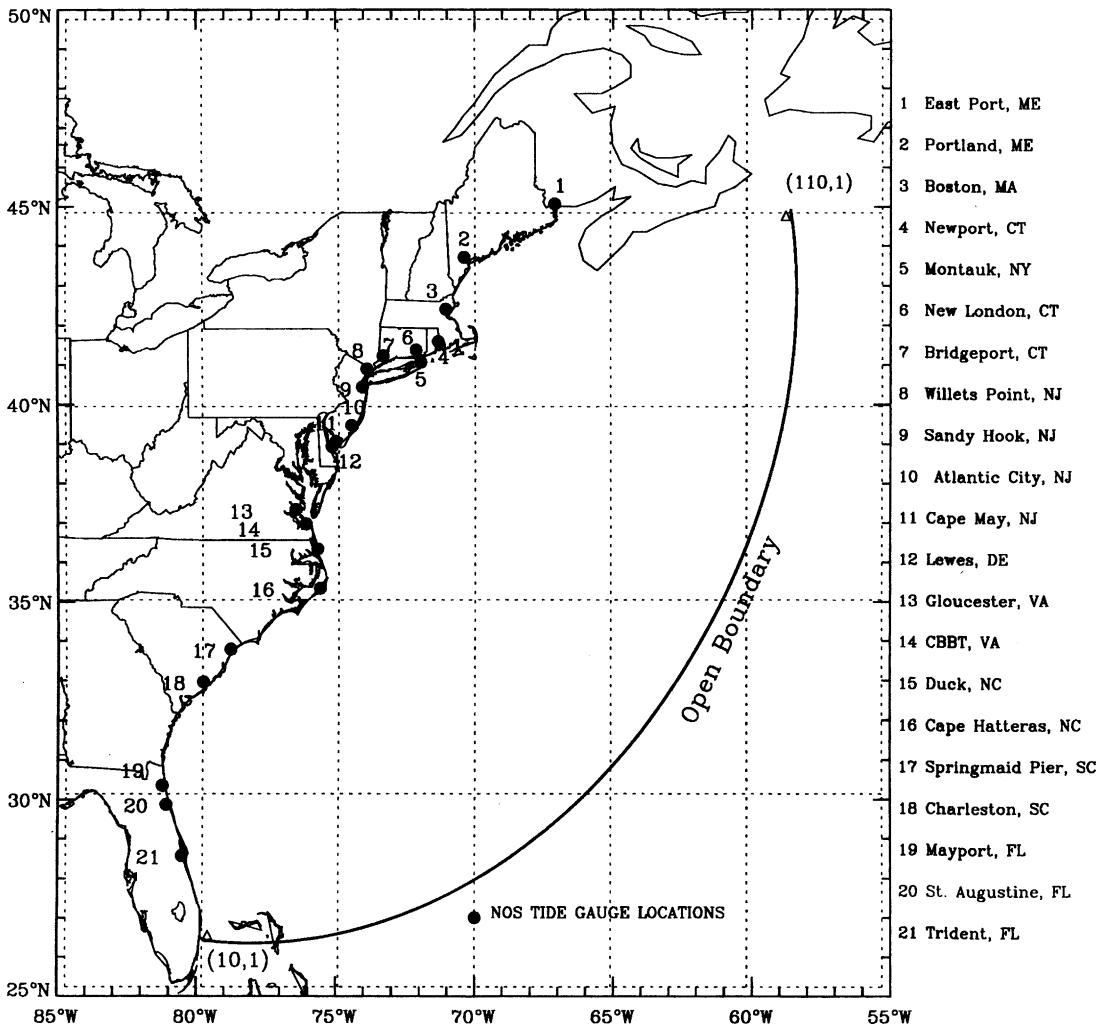

Fig. 1. Locations of 21 tide gauge stations from National Water Level Observation Network (NWLON) that are used in this study.

Table 1
Scale factors for the amplitude and phase of the five major tidal constituents

Constituent	f_1	f_2	f_3	f_4	f_5	f_6
M_2	1	10^{-2}	10^{-4}	10^{2}	1	10^{-3}
S_2	10^{-1}	10^{-3}	10^{-5}	10^{2}	1	10^{-3}
N_2	10^{-1}	10^{-3}	10^{-5}	10^{3}	1	10^{-2}
K_1	10^{-1}	10^{-3}	10^{-5}	10^{3}	1	10^{-3}
O_1	10^{-1}	10^{-5}	10^{-5}	10^{3}	1	10^{-4}

scale factors, f_1–f_6 (Table 1) so that all control variables have the same order in magnitude and similar weight during the optimization. This avoids ill-conditioning of the Hessian matrix which is used in minimization algorithms such as the quasi-Newton method.

2.3. Adjoint equations

In this study, discrete adjoint equations were directly constructed from the discrete nonlinear two-dimensional POM forward equations (Zhang et al., 2002b). For clarity, construction of the adjoint equations is briefly summarized in continuous notation in this paper. Augmented Lagrange function is formulated by introducing

Lagrangian multipliers λ_h, λ_u and λ_v for the constraint equations and open boundary conditions (Lawson et al., 1995). The first-order variational of the cost function was written as

$$\begin{aligned}\delta J = &\int\int\int_{xyt}(h_m - h_0)\,\mathrm{d}x\,\mathrm{d}y\,\mathrm{d}t \\ &+ \int\int_{xt}\lambda_h\delta h_{j=1}(t)\,\mathrm{d}x\,\mathrm{d}t \\ &+ \int\int\int_{xyt}\lambda_h\delta(\text{left-hand side of Eq. (1)}) \\ &\times \mathrm{d}x\,\mathrm{d}y\,\mathrm{d}t + \int\int\int_{xyt}\lambda_u\delta \\ &\times (\text{left-hand side of Eq. (2)}) \\ &\times \mathrm{d}x\,\mathrm{d}y\,\mathrm{d}t + \int\int\int_{xyt}\lambda_v\delta \\ &\times (\text{left-hand side of Eq. (3)}) \\ &\times \mathrm{d}x\,\mathrm{d}y\,\mathrm{d}t. \end{aligned} \tag{13}$$

The corresponding adjoint variables are defined as follows: λ_h is the adjoint variable of h, λ_u is the adjoint variable of U, and λ_v is the adjoint variable of V, respectively. After applying the chain rule, integrating by parts and regrouping, Eq. (13) is rewritten as

$$\begin{aligned}\delta J = &\int\int\int_{xyt}\left(h_m - h_0 - \frac{\partial\lambda_h}{\partial t} - g\frac{\partial D\lambda_u}{\partial x} - g\frac{\partial D\lambda_v}{\partial y}\right)\delta h\,\mathrm{d}x\,\mathrm{d}y\,\mathrm{d}t \\ &+ \int\int\int_{xyt}\begin{pmatrix} -D\dfrac{\partial\lambda_u}{\partial t} - D\dfrac{\partial\lambda_h}{\partial x} - 2UD\dfrac{\partial\lambda_u}{\partial x} - \dfrac{\partial}{\partial x}\left(2DA_M\dfrac{\partial\lambda_u}{\partial x}\right) - DV\dfrac{\partial\lambda_u}{\partial y} \\ -\dfrac{\partial}{\partial y}\left(DA_M\dfrac{\partial\lambda_u}{\partial y}\right) - \dfrac{C_b\lambda_u}{\rho}\dfrac{2U^2+V^2}{\sqrt{U^2+V^2}} - \dfrac{\partial}{\partial y}\left(DA_M\dfrac{\partial\lambda_v}{\partial x}\right) - VD\dfrac{\partial\lambda_v}{\partial x} \\ +(f+\tilde{f})D\lambda_v + (U\lambda_v - V\lambda_u)D\dfrac{\delta_y(\Delta x)}{\Delta x\,\Delta y} - \dfrac{C_b\lambda_v}{\rho}\dfrac{UV}{\sqrt{U^2+V^2}} \end{pmatrix}\delta U\,\mathrm{d}x\,\mathrm{d}y\,\mathrm{d}t \\ &+ \int\int\int_{xyt}\begin{pmatrix} -D\dfrac{\partial\lambda_v}{\partial t} - D\dfrac{\partial\lambda_h}{\partial y} - UD\dfrac{\partial\lambda_u}{\partial y} - \dfrac{\partial}{\partial x}\left(DA_M\dfrac{\partial\lambda_u}{\partial y}\right) - 2VD\dfrac{\partial\lambda_v}{\partial y} \\ -\dfrac{\partial}{\partial y}\left(2DA_M\dfrac{\partial\lambda_v}{\partial y}\right) - \dfrac{C_b\lambda_v}{\rho}\dfrac{U^2+2V^2}{\sqrt{U^2+V^2}} - \dfrac{\partial}{\partial x}\left(DA_M\dfrac{\partial\lambda_v}{\partial x}\right) - UD\dfrac{\partial\lambda_v}{\partial x} \\ -(f+\tilde{f})D\lambda_u + (V\lambda_u - U\lambda_v)D\dfrac{\delta_x(\Delta y)}{\Delta x\,\Delta y} - \dfrac{C_b\lambda_u}{\rho}\dfrac{UV}{\sqrt{U^2+V^2}} \end{pmatrix}\delta V\,\mathrm{d}x\,\mathrm{d}y\,\mathrm{d}t \\ &+ \int\int_{it}\lambda_h\delta h_i(t)\,\mathrm{d}i\,\mathrm{d}t. \end{aligned} \tag{14}$$

By forcing the coefficients of the noncontrol variables (δh, δU and δV) of Eq. (14) in interior of the model domain to zero, the corresponding adjoint equations are as follows:

$$\frac{\partial\lambda_h}{\partial t} + g\frac{\partial D\lambda_u}{\partial x} + g\frac{\partial D\lambda_v}{\partial y} = h_m - h_0, \tag{15}$$

$$\begin{aligned} &D\frac{\partial\lambda_u}{\partial t} + 2UD\frac{\partial\lambda_u}{\partial x} + VD\left(\frac{\partial\lambda_u}{\partial y} + \frac{\partial\lambda_v}{\partial x}\right) \\ &+ \frac{\partial}{\partial x}\left(2DA_M\frac{\partial\lambda_u}{\partial x}\right) + \frac{\partial}{\partial y}\left(DA_M\left(\frac{\partial\lambda_u}{\partial y} + \frac{\partial\lambda_v}{\partial x}\right)\right) \\ &- (f+\tilde{f})D\lambda_v - (U\lambda_v - V\lambda_u)D\frac{\delta_y(\Delta x)}{\Delta x\,\Delta y} \\ &+ \frac{C_b}{\rho}\left(\lambda_u\frac{2U^2+V^2}{\sqrt{U^2+V^2}} + \lambda_v\frac{UV}{\sqrt{U^2+V^2}}\right) \\ &+ D\frac{\partial\lambda_h}{\partial x} = 0, \end{aligned} \tag{16}$$

$$\begin{aligned} &D\frac{\partial\lambda_v}{\partial t} + UD\left(\frac{\partial\lambda_u}{\partial y} + \frac{\partial\lambda_v}{\partial x}\right) + 2VD\frac{\partial\lambda_v}{\partial y} \\ &+ \frac{\partial}{\partial x}\left(DA_M\left(\frac{\partial\lambda_u}{\partial y} + \frac{\partial\lambda_v}{\partial x}\right)\right) + \frac{\partial}{\partial y}\left(2DA_M\frac{\partial\lambda_v}{\partial y}\right) \end{aligned}$$

$$+(f+\tilde{f})D\lambda_u+(V\lambda_u-U\lambda_v)D\frac{\delta_x(\Delta y)}{\Delta x\,\Delta y}+\frac{C_b}{\rho}\times\left(\lambda_u\frac{UV}{\sqrt{U^2+V^2}}+\lambda_v\frac{U^2+2V^2}{\sqrt{U^2+V^2}}\right)+D\frac{\partial\lambda_h}{\partial y}=0 \quad (17)$$

the variational of the cost function can be written as

$$\delta J=\int\int_{x,t}\lambda_h\delta h_{j=1}(t)\,\mathrm{d}x\,\mathrm{d}t. \quad (18)$$

If only one tidal constituent is used as open boundary forcing, substitute Eqs. (9), (11) and (12) into Eq. (18), the gradients of the cost function with respect to the control variables are represented as

$$\begin{aligned}
\frac{\partial J}{\partial a_1}&=\int\int_{i,t}\gamma\lambda_h(i,t)\cos(\omega t+E-\Theta_i)\,\mathrm{d}i\,\mathrm{d}t,\\
\frac{\partial J}{\partial a_2}&=\int\int_{i,t}\gamma\lambda_h(i,t)i\cos(\omega t+E-\Theta_i)\,\mathrm{d}i\,\mathrm{d}t,\\
\frac{\partial J}{\partial a_3}&=\int\int_{i,t}\gamma\lambda_h(i,t)i^2\cos(\omega t+E-\Theta_i)\,\mathrm{d}i\,\mathrm{d}t,\\
\frac{\partial J}{\partial a_4}&=\int\int_{i,t}\gamma\lambda_h(i,t)A_i\sin(\omega t+E-\Theta_i)\,\mathrm{d}i\,\mathrm{d}t,\\
\frac{\partial J}{\partial a_5}&=\int\int_{i,t}\gamma\lambda_h(i,t)A_ii\sin(\omega t+E-\Theta_i)\,\mathrm{d}i\,\mathrm{d}t,\\
\frac{\partial J}{\partial a_6}&=\int\int_{i,t}\gamma\lambda_h(i,t)A_ii^2\sin(\omega t+E-\Theta_i)\,\mathrm{d}i\,\mathrm{d}t.
\end{aligned} \quad (19)$$

Eq. (19) can be applied to every tidal constituent (M_2, S_2, N_2, K_1, O_1). The total number of the control variable is determined by how many tidal constituents are prescribed on the open boundary.

3. Assimilation experiments

The procedure of an iterative optimal data assimilation that is applied to all the following data assimilation experiments is described as:

(i) Run forward numerical model for 30 days (which is called data assimilation window) with initial values of the control variables, and save the simulated elevations at the corresponding tidal gauge locations at every hour.

(ii) Calculate data misfits between the simulated results (h_m) and the predicted tidal elevations (h_0) at locations where data exist and save them into a temporary file. Calculate values of the cost function with Eq. (10).

(iii) Run adjoint model backwards in time forced by the data misfits to calculate the adjoint variables. Then calculate the gradient of the cost function with respect to the control variables using the adjoint variables.

(iv) Employ the limited memory BGFS quasi-Newton minimization algorithm (Liu and Nocedal, 1989) to update optimal control variable estimates.

(v) Check whether the convergence criterion, $|G|<\varepsilon$ or $J<\varepsilon$ (J and G are values of the cost function and its gradient with respect to the control variables, $\varepsilon=10^{-6}$), for the minimization process is satisfied. If Yes, iteration is stopped. Otherwise, steps (i)–(v) are repeated with the new parameter estimates.

(vi) Run forward numerical model with the final optimal open boundary conditions.

3.1. Identical twin experiments

Identical twin experiment techniques are the most useful tools to verify and evaluate the performance and feasibility of the adjoint data assimilation procedure. In an identical twin experiment, pseudo-observations are generated by the numerical model with a set of predetermined control variables so that the observations are (by definition) not contaminated by any error and contain the same dynamics as the numerical model. All kinds of pseudo-observations (current and elevation) may be sampled at any grid point and any time step. Another merit of the identical twin experiment is that since the true values of control variables are known, one can therefore test whether or not the calculated values of the optimal control variables converge to their true values. Thus, the identical twin experiment is widely used to evaluate and verify the performance of developed adjoint data assimilation systems. Here the

M_2 tidal constituent is used as an example for the identical twin experiments in which elevations of M_2 constituent are calculated from the predetermined control variables and are prescribed along the open boundary. The tidal model is integrated with the predetermined values of a_1–a_6 (called "true" values of the control variables) for at least 60 days (the data of the first 30 days of spinup are not used). The simulated elevations at 21 grid locations that coincide with NOS's tide gauge locations are saved hourly and used as the pseudo-observations in the data assimilation process.

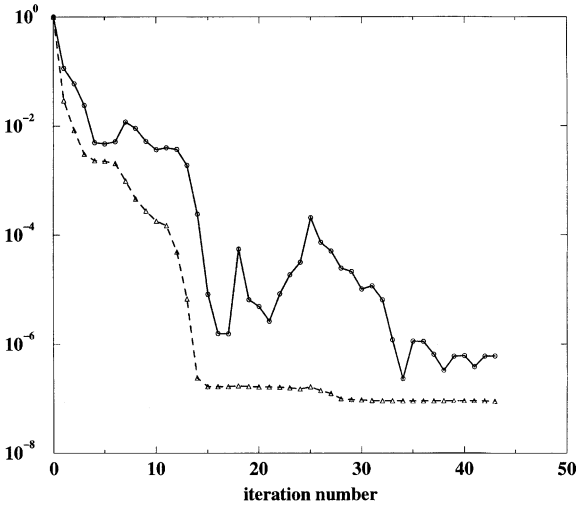

Fig. 2. Values of gradient norm and cost function versus iteration number for the twin experiment (M_2). Solid line, G/G_0; dotted line, J/J_0.

The first identical twin experiment was conducted with the initial values of the control variables obtained by adding 0.5 to their true values. Fig. 2 shows the values of the cost function and the norm of its gradients versus the number of iterations in an optimization process (all values are normalized by their own initial values J_0 and G_0). We can see that the cost function and the norm of the gradient drop rapidly in the first several iterations, and the convergence criterion is satisfied after 43 iterations. The relative values of the cost function (J/J_0) decrease from 1 to 10^{-7}.

The final value of the norm of the gradient is less than 10^{-6}. The optimal amplitudes and phases of the M_2 constituent along the open boundary (Fig. 3) converge closely to their true values from the initial values. The RMS errors between the true and optimal elevations for 30 days at the open

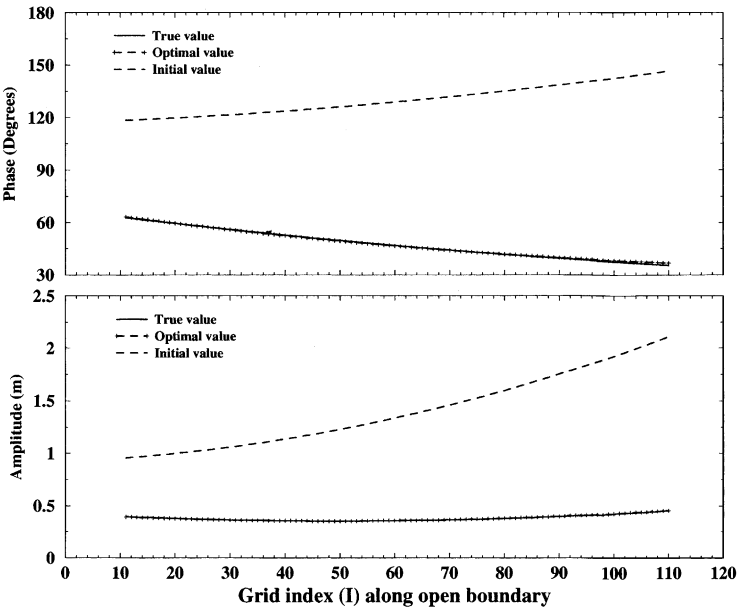

Fig. 3. True, initial and computed (optimal) amplitudes and phases along the open boundary for the twin experiment for M_2.

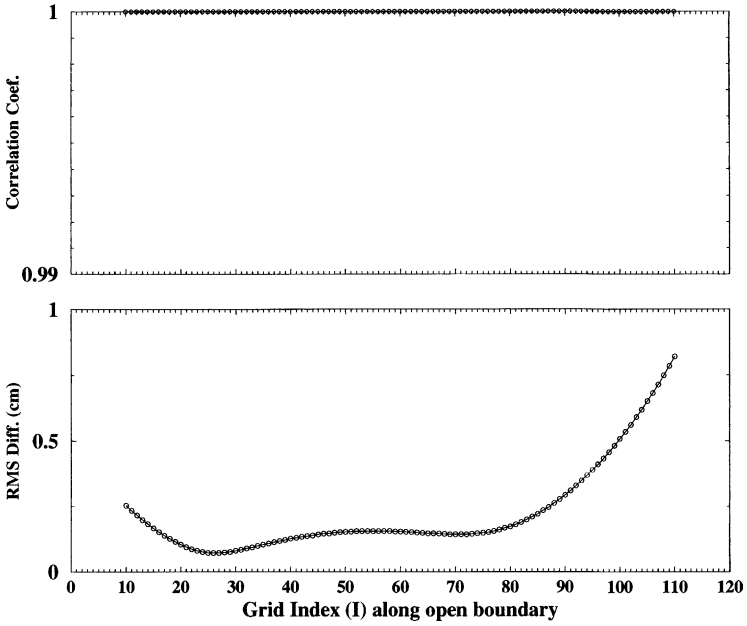

Fig. 4. Correlation coefficients and RMS errors (centimeters) between the true open boundary elevations and the optimal open boundary elevations.

boundary are calculated and presented in Fig. 4. It is shown that, although the optimal amplitude and phase are not exactly coincident with the true values, the RMS errors in the water levels are less than 1 cm and the correlation coefficients are greater than 0.999. Another experiment with zeros as initial values of the control variables was conducted to test the sensitivity of the performance of the optimization procedure to the initial values. Similar results as the previous experiment were obtained. This shows that the optimization procedure is independent of the choice of the initial guess. However, the initial guess must be meaningful and allow the model to run reasonably. A good initial guess may reduce the iteration number of the optimization process, so the initial values of the control variables should be as close to the true solution as possible.

A series of experiments, in which the number of tide gauges used in data assimilation is reduced step by step, are now discussed to investigate the effect of the amount of observations on the optimization procedure. We start with all 21 gauge stations (denoted by Sta21) in which the pseudo-observations from the 21 tide gauge stations are assimilated. In the next experiment, the nine tide gauge stations which are located at open coast are selected from Sta21 (the station numbers are 5, 9, 10, 12, 15, 16, 18, 20 and 21) and the pseudo-observations at these nine tide gauge stations are assimilated (Sta9). In Sta6, six stations are selected from the stations used in experiment Sta9 (the station numbers are 5, 9, 10, 15, 16 and 20). The first guess of each control variable is the same in all experiments (increased by 0.5 on its own true value). Optimal values of the control variables for the three experiments are listed in Table 2 and the optimal harmonic constants for the M_2 (amplitude and phase) along the open boundary derived from the optimal values of the control variables for the above three experiments are presented in Fig. 5. The figure shows that the optimal control parameters are not exactly equal to the true values for the three experiments and that there are minimal differences between them. The optimal control variables from Sta9 are very close to those from Sta21 (the difference of each control variable is less than 0.004). The optimal amplitudes and phases along the open boundary derived by the optimal control variables from Sta21 and Sta9 are almost

coincident and are the closest to the true values among all the experiments. The simulated elevations at the tidal gauge stations from these experiments are all very close to the pseudo-observations (the RMS errors at 21 tidal stations for the three experiments are less than 0.1 cm). This demonstrates that the true open boundary elevations can be recovered by assimilating tidal elevations at coastal stations. It is noted (Table 2) that the parameter a_6 did not converge to its true value from the initial value for all these experiments (keep its initial value). The reason might be that the true phase solution looks much like a linear function of i, so the model simulations are not sensitive to a_6. It makes little sense to try to determine this parameter, the parameter a_6 can be specified as a constant or is discarded in data assimilation procedure.

Table 2
Optimal coefficients of the quadratic polynomials of amplitude and phase of M_2 constituent for the twin identical experiments

	a_1	a_2	a_3	a_4	a_5	a_6
True	0.4213	−0.2759	0.2769	0.6688	−0.3929	0.9759
Initial	0.9213	0.2241	0.7769	1.1688	0.1071	1.4759
Sta21	0.4187	−0.2695	0.2764	0.6771	−0.4339	1.4349
Sta9	0.4189	−0.2699	0.2767	0.6768	−0.4386	1.4370
Sta6	0.4131	−0.2377	0.2446	0.6734	−0.4305	1.4421
Sta9_2	0.4096	−0.2160	0.2221	0.6703	−0.4240	1.4430
Sta6_2	0.4076	−0.2313	0.2453	0.6794	−0.4423	1.4272

In order to investigate the effect of the distribution of assimilated data stations on the optimization procedure, two other experiments have been performed: Sta9_2 and Sta6_2. In Sta9_2 experiment, the data from the nine tide gauge stations of 4, 6, 7, 8, 11, 13, 14, 17, 19 (which are located inside of bays and not used in the experiment Sta9) are assimilated. In Sta6_2 experiment, to test the influence of northern locations, data from six consecutive stations between Montauk and Lewes (station numbers from 7 to 12) are assimilated. The resulting optimal amplitude and phase at the open boundary are also plotted in Fig. 5. The optimal amplitude and phase at the open boundary from Sta9_2 deviated farther away from the true values even than that of Sta6. This shows that the data from inside bays or inside rivers may include some signals that cannot be produced by the open boundary tidal forcing. Thus, the real open boundary conditions may not be obtained by

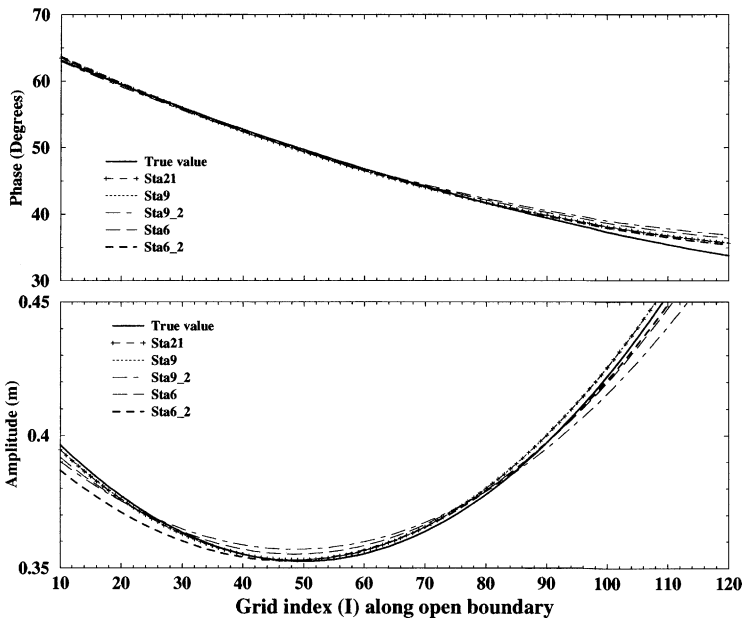

Fig. 5. True and optimal amplitudes (meters) and phases (degrees relative to GMT) at the open boundary from different twin experiments (M_2). Increasing index is from south to north (see Fig. 1).

assimilating the data from inside shallow bays. In Sta6_2, the data from some of the northern six stations of Sta21 are used. The optimal amplitudes and phases at the northeastern part of the open boundary are the closest to the true values among the results of all twin experiments. However, the worst results are obtained for the southern part of the open boundary, indicating that the true open boundary at the southern region might not be accurately recovered when only using tide gauge stations from the northern region.

3.2. Practical application

3.2.1. Experimental methodology

Two practical application experiments denoted as the individual tidal constituent estimation (PA_ITC) and the combined tidal constituents estimation (PA_CTC) were performed. For the first (PA_ITC), the same data assimilation procedure as that of the identical twin experiment Sta9 is individually applied for each of the five tidal constituents to obtain their optimal harmonic constants. It is noted that five control variables in total were used for each constituent within each data assimilation process based on the results of the identical twin experiments (model simulation is not sensitive to a_6). The optimal harmonic constants of these five tidal constituents from the separate data assimilation processes are then combined and used as the lateral open boundary conditions for a new simulation run. For PA_CTC, the harmonic constants of the five tidal constituents are estimated in a single data assimilation process (25 control variables in total). Thus the interaction effects of the tidal constituents are included while the tides propagate into shallow coastal region where nonlinear effects begin to become important. The twin experiments showed that the experiment Sta9 in which the data from the nine coastal stations were assimilated achieved almost the same results as the experiment Sta21. Since topography and geometry inside bays or rivers cannot be well resolved by the present model grid resolution, this may cause the model results at grid points inside shallow bays not to match the corresponding observations well. Therefore, tidal predicted elevations (calculated by using the harmonic constants of the corresponding NOS-accepted constituents) from the nine stations of Sta9 are used in the data assimilation process, and the elevations from the other stations are used for comparison. Since the harmonic constants from Schwiderski's global tide model and the global tidal inverse model of Oregon State University are very similar along the open boundary, the harmonic constants of each tidal constituent from Schwiderski's global tide model are interpolated along the open boundary and then used as initial values for the control variables.

3.2.2. Results

Optimal control variables: The resulting optimal quadratic polynomial coefficients of the amplitude and phase from experiment PA_ITC are listed in Table 3. The optimal harmonic constants (amplitude and phase) of these five major tidal constituents along the open boundary are compared with the initial values from Schwiderski's global tide model in Fig. 6. It can be seen that the optimal amplitudes of the M_2, S_2, K_1 and O_1 constituents along the open boundary from the two data assimilation experiments PA_CTC and PA_ITC are close (the differences are generally less than 2 cm for M_2, and 0.3 cm for S_2, K_1 and O_1), but PA_CTC is about 2 cm greater than PA_ITC for N_2. The curve shapes of the optimal amplitudes of M_2, S_2 are similar to those of Schwiderski's global tide model results. The optimal phases of M_2 from the two experiments are very close (less then 2°) and smaller than those of Schwiderski's global tide model from 5° at southwest to 20° at northeast. The differences in the optimal phases of S_2 and N_2

Table 3
Optimal quadratic polynomial coefficients for the amplitude and phase of the five major tidal constituents from experiment PA_ITC

Constituent	a_1	a_2	a_3	a_4	a_5
M_2	0.409	−0.301	0.332	0.123	−0.385
S_2	0.601	−0.384	0.889	0.321	−0.279
N_2	0.819	−0.585	0.546	0.341	−0.230
K_1	0.870	−0.202	0.060	0.206	−0.274
O_1	0.568	0.726	−0.217	0.230	−0.442

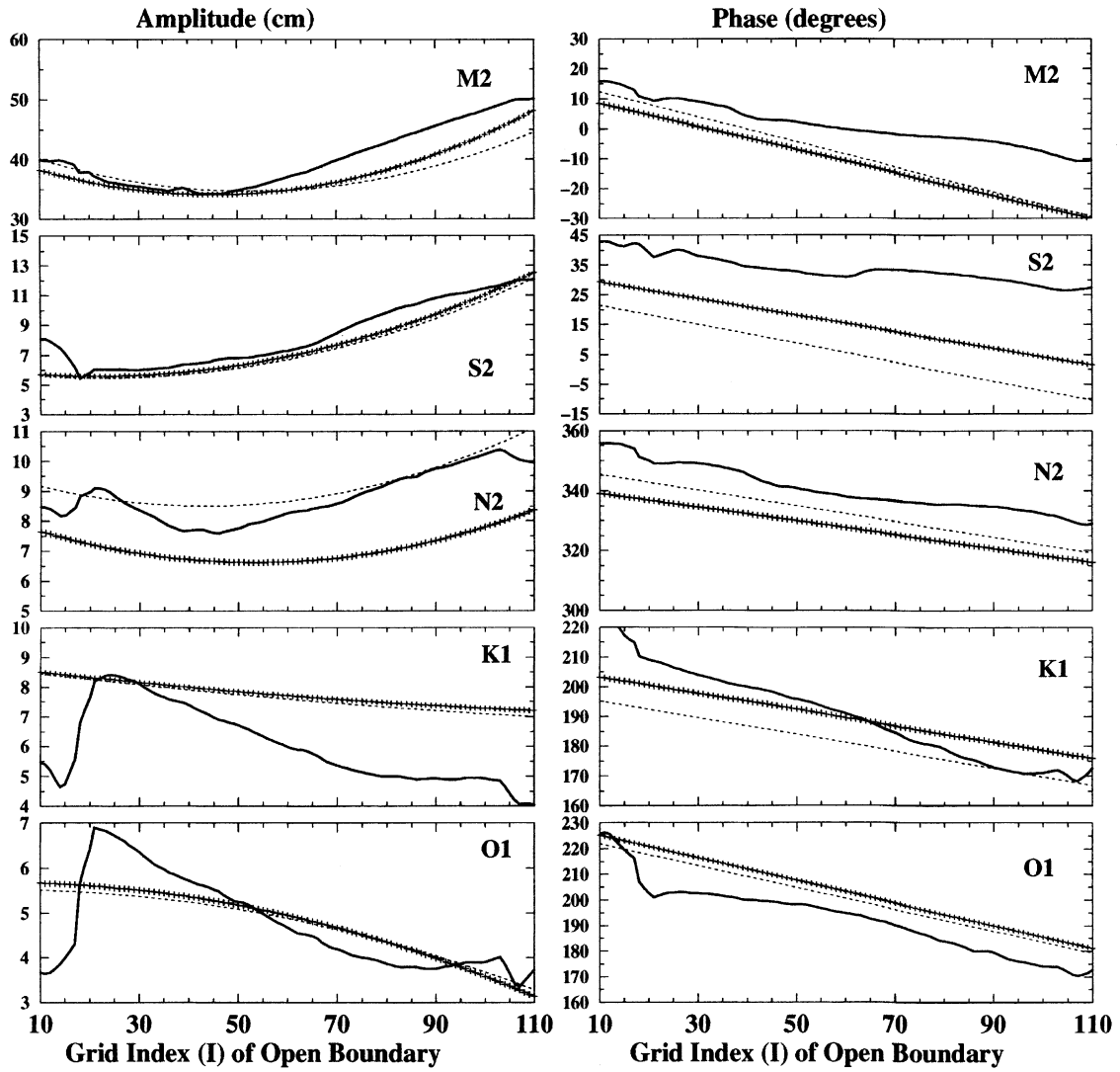

Fig. 6. Amplitudes (centimeters) and phases (degrees relative to GMT) from Schwiderski global tide model and the optimal data assimilation experiments. Solid line, from Schwiderski global model; dashed line with plus, from PA_ITC; dotted line, from PA_CTC.

between the two experiments PA_ITC and PA_CTC are generally 10°, and they are smaller than those of Schwiderski's global tide model results. The differences in the optimal phases of O_1 from the two experiments are less than 2°, and they are generally 10° greater than those of Schwiderski's model results.

Correlation coefficients and RMS errors: RMS errors and correlation coefficients between the tidal predictions and the simulated elevations are plotted in Fig. 7. The RMS errors with the open boundary conditions from Schwiderski's tidal model are generally smaller than 15 cm at the coastal tide gauge locations, while the correlation coefficients are greater than 0.9. It may show that the Schwiderski's tidal model results in deep waters can be generally used as open boundary conditions for a regional tidal model (as expected for a regional ocean model). For the data assimilation experiments PA_ITC and PA_CTC, both the RMS errors and correlation coefficients are close (the differences less than 2 cm and 0.01,

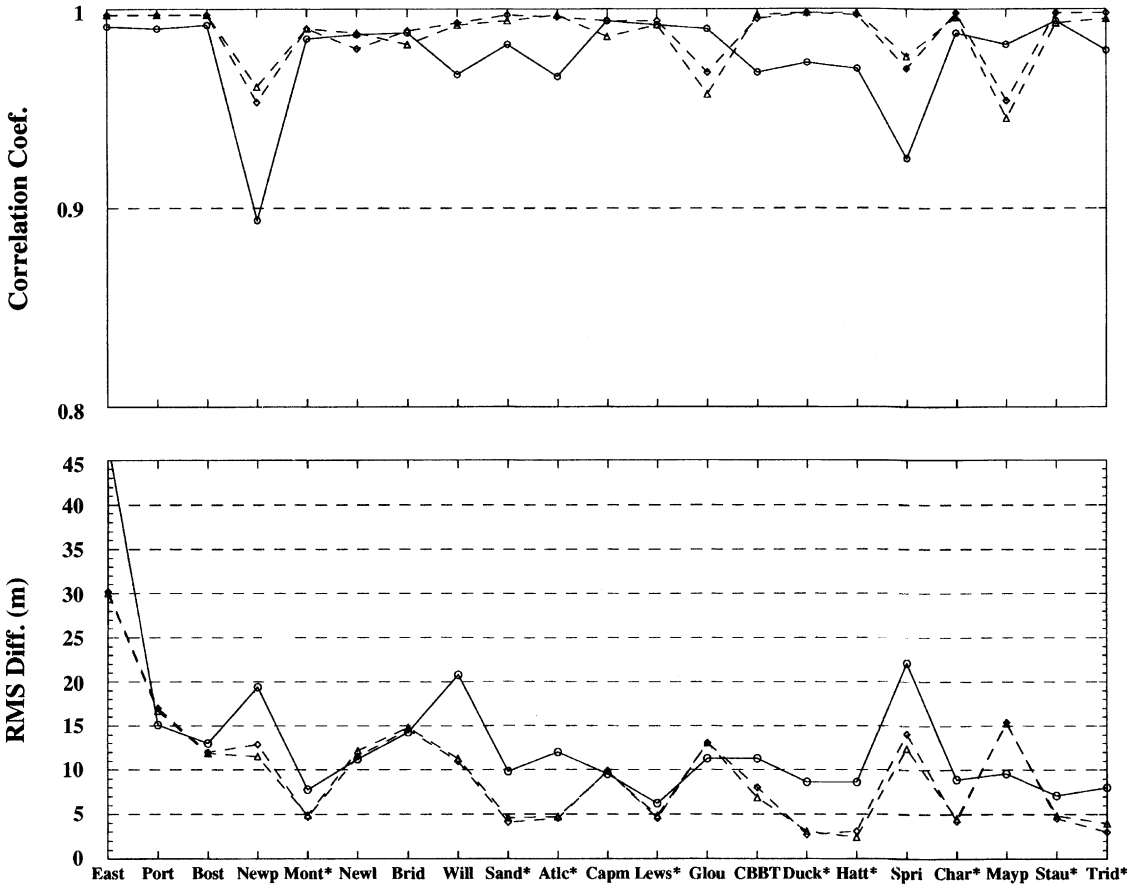

Fig. 7. RMS errors and correlation coefficients between the tidal predictions and model results with open boundary conditions from Schwiderski global tide model and the optimal data assimilation experiments. Solid line with circle, Schwiderski global model; dashed line with triangle up, from PA_ITC; dashed line with diamond, from PA_CTC. The asterisk beside the station name indicates that the data from that station were used in assimilation.

respectively). The maximum RMS error is 30 cm at Eastport, and the minimum correlation coefficient is 0.96 at Mayport. The RMS errors are less than 5 cm and the correlation coefficients are greater than 0.99 for the nine coastal stations used in the data assimilation procedure. For most of the stations, the RMS errors with the optimal boundary conditions are smaller than those with the open boundary conditions from Schwiderski's model results and correlation coefficients are greater. At Mayport and Gloucester, RMS errors with the open boundary conditions from Schwiderski's model results are smaller and the correlation coefficients are greater. The assimilation model does worse at tide gauges inside a bay, with the RMS errors growing as one goes further up the bay. For example, the RMS error grows as one moves up Long Island Sound, from Montauk to New London to Bridgeport. The RMS error also grows as one moves up the Golf of Maine, from Boston to Portland to Eastport. Here the error becomes quite large because no other tide gauge stations were used for the Gulf of Maine in the assimilation, especially from the bay of Fundy area with its huge tidal ranges. Other inside stations (Newport, Gloucester, Springmaid Pier, and Mayport) also have larger errors than nearly coastal stations.

Time series and cotidal charts: Comparison between the time series of the simulated elevations

from PA_ITC and PA_CTC at costal locations shows that there are no significant differences between them (RMS difference is generally less than 2 cm). Although there are some differences among the optimal amplitudes and phases for each tidal constituent along the open boundary of the two experiments, the combined optimal open boundary elevations for these two experiments are almost the same. The simulated elevations forced by the optimal open boundary conditions from these two experiments are therefore coincident. However, PA_CTC simulations are less computationally expensive than PA_ITC (computational time was reduced by 70%). Time series of tidal predictions and model results from the experiments with the open boundary conditions from PA_CTC and Schwiderski global tidal model are plotted in Fig. 8. They show that the model simulated elevations with open boundary conditions from Schwiderski tidal model are generally close to the tidal predictions (the RMS errors are less than 15 cm, except at Eastport, Newport, Willets Point and Springmaid), but the phases of the model results are generally delayed. The simulated elevations with the optimal open boundary conditions match the tidal predictions better than those with the open boundary conditions from Schwiderski tidal model.

Coamplitudes and cophases of the five constituents were calculated by analyzing 1-year simulated elevations from experiment PA_CTC using a least squares method and presented in Fig. 9 (O_1 is not shown since it has a pattern similar to that of K_1). For the semi-diurnal constituents M_2, S_2 and N_2, the amplitudes in the deep waters increase from southwest to northeast. The amplitudes of M_2 are less than 1 m except inside of the Gulf of Maine where amplitudes exceed 2 m, and the amplitudes of S_2 and N_2 are generally in the range of 8–20 cm except inside of the Gulf of Maine where they exceed 20 cm. The phases of M_2 and N_2 in the deep waters are generally consistent from south to north, while the phases of S_2 in the deep waters increase from south to north. The diurnal K_1 and O_1 have similar amplitude and phase patterns. Amplitudes are generally not more than 10 cm and phases decrease from south to north. The computed and the corresponding NOS-

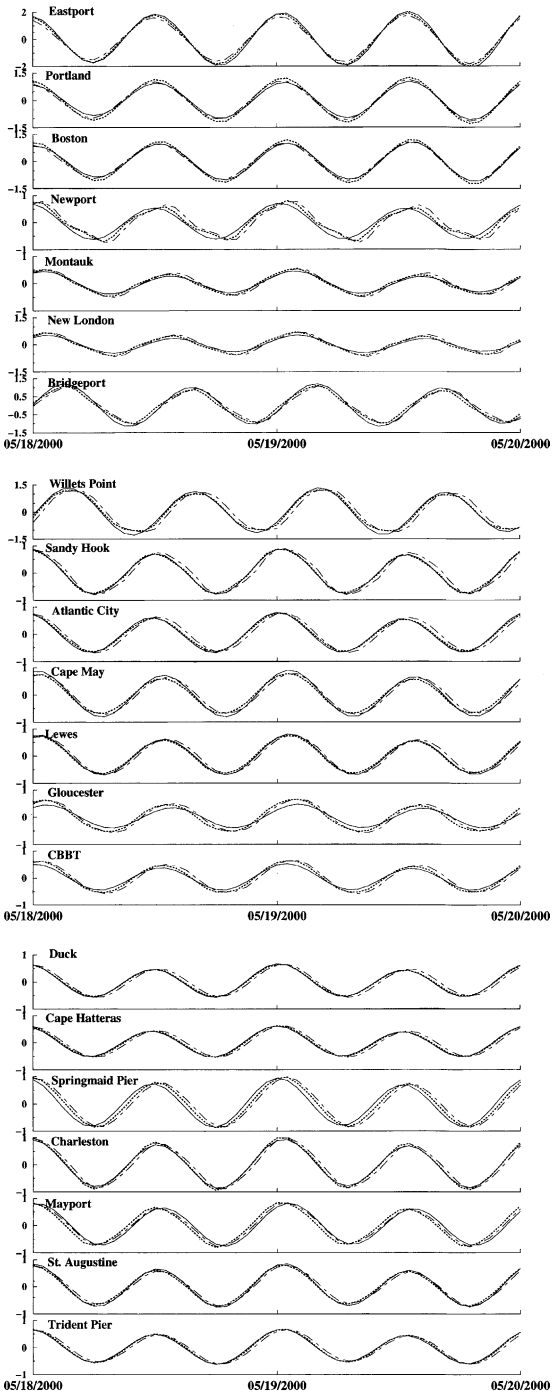

Fig. 8. Tidal predictions (solid line) compared to model results with open boundary conditions from Schwiderski tide model (dot-dashed line) and the data assimilation experiment PA_CTC (dotted thick line).

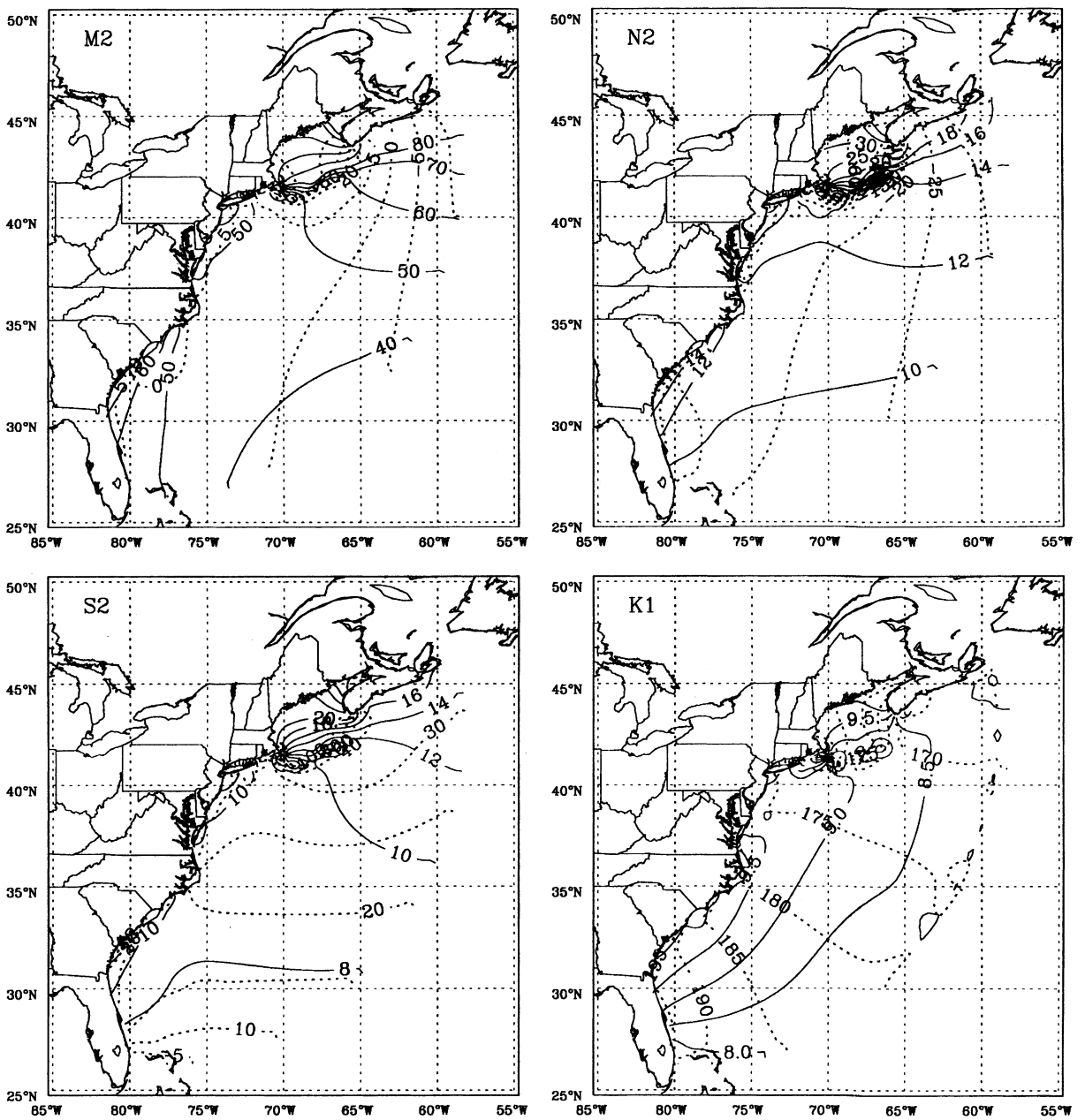

Fig. 9. Cotidal charts of M_2, S_2, N_2, K_1 constituents based on the model results of PA_CTC (with optimal tidal open boundary conditions). Solid line, coamplitudes (in centimeters); dotted line, cophases (in degrees relative to GMT).

analyzed tidal harmonic constants at 18 tide gauge stations (listed in Table 4) show that, for the M_2 constituent, the maximum amplitude error is 8 cm (at New London station), and the amplitude errors are less than 5 cm at the open coast stations. The maximum phase error is 10° (at Sandy Hook). The maximum amplitude differences for the S_2, N_2, K_1 and O_1 constituents are 3.1, 3.4, 5

Table 4
Comparison of NOS-analyzed and computed (PA_CTC) harmonic constants (amplitude A, in centimeters and local phase, θ, in degrees relative to GMT) of M_2, S_2, N_2, K_1, O_1 at 21 tide gauge locations

Station	M_2				S_2				N_2				K_1				O_1			
	Obs.		MODEL		Obs.		MODEL		Obs.		MODEL		Obs.		MODEL		Obs.		MODEL	
	A	θ	A	θ	A	θ	A	θ	A	θ	A	θ	A	θ	A	θ	A	θ	A	θ
Eastport	268.7	98	229.0	98	42.9	138	35.1	136	56.2	68	46.4	66	15.4	196	10.9	184	11.8	177	8.4	184
Portland	136.5	102	147.8	100	21.3	138	22.9	139	31.3	72	31.6	70	14.0	201	10.0	193	11.3	182	3.7	320
Boston	139.5	109	141.5	108	22.0	146	20.6	151	30.7	77	30.3	79	15.0	205	10.0	197	11.9	186	7.9	193
Newport	52.9	1	58.5	1	12.3	23	10.1	34	12.7	344	14.4	348	6.4	168	8.5	169	5.1	198	6.3	175
Montauk	29.6	47	33.5	44	6.5	58	5.4	60	7.9	23	8.6	15	7.3	179	8.0	186	5.1	207	5.9	188
New London	36.6	58	44.7	53	7.2	69	6.7	73	8.9	34	10.2	25	7.5	179	8.4	187	5.2	203	6.2	190
Bridgeport	98.5	108	90.2	105	16.6	134	13.2	135	21.5	86	18.1	78	9.1	191	10.1	204	6.6	218	7.3	206
Willets Point	113.5	116	115.6	116	18.6	141	17.3	148	23.0	91	23.2	91	9.8	192	11.0	209	6.4	229	7.8	210
Sandy Hook	69.3	7	68.5	17	13.7	35	11.5	44	15.7	350	16.5	357	10.5	175	9.8	181	5.4	171	7.5	180
Atlantic City	60.1	356	58.9	1	11.9	20	9.8	33	14.0	336	14.4	347	11.2	181	9.3	177	7.7	167	7.3	179
Cape May	72.2	28	68.0	27	12.7	56	10.8	55	15.8	9	15.6	7	10.9	199	9.6	185	8.3	185	7.3	186
Lewes	61.5	31	63.9	31	10.9	56	10.1	58	13.2	8	14.8	10	10.4	202	9.4	187	8.7	189	7.2	189
CBBT	39.4	21	39.1	27	7.4	47	6.6	49	8.9	2	10.0	9	5.9	186	10.4	188	4.7	206	7.7	189
Duck	49.1	359	47.4	6	9.3	23	7.6	28	11.5	338	11.6	345	9.2	175	9.2	177	6.1	190	7.1	180
Cape Hatteras	45.3	353	45.8	1	8.2	16	7.1	21	10.6	331	11.1	343	9.4	185	9.8	180	7.5	186	6.6	196
Springmaid	75.1	357	78.1	359	13.6	21	11.4	17	17.4	340	17.4	345	10.3	189	10.5	188	7.7	193	8.0	196
Charleston	75.8	17	79.8	14	13.1	39	10.9	36	16.7	359	16.5	6	10.4	202	10.5	199	7.8	205	7.6	208
Mayport	66.2	28	69.9	7	11.1	52	10.9	24	14.9	10	14.0	352	8.2	204	9.8	196	6.0	212	6.8	205
St. Augustine	66.2	14	66.1	7	11.2	36	10.2	23	16.3	355	13.1	352	10.1	197	9.6	196	7.3	202	6.6	205
Trident	51.7	7	53.7	6	8.1	28	8.5	19	11.9	348	11.1	351	10.1	202	8.9	197	7.7	205	5.9	206

and 4 cm while the maximum phase differences are 28°, 18°, 17° and 23°.

4. Summary

An adjoint data assimilation model was developed using tidal harmonic constants (amplitude and phase) along the open boundary as control variables and defining the cost function by the tidal elevation misfits at selected tide gauge stations. The number of control variables was reduced by approximating the harmonic constants at the open boundary with a quadratic polynomial formulation.

Identical twin experiments were performed to verify and evaluate the performance and feasibility of the adjoint data assimilation procedure. The results showed that the true open boundary conditions were well recovered by assimilating ideal pseudo-observations from several coastal stations. Better results were obtained by assimilating the data from open coast stations than from those located inside shallow bays or shallow rivers. Also, the more uniform the spatial distribution of the stations, the better the optimal open boundary conditions that were obtained. The optimization procedure is independent of the choice of the initial guesses of the control variables.

The experiments of real tidal data assimilation, the tidal predicted elevations at nine coastal stations were assimilated into the numerical model and the harmonic constants from Schwiderski global tidal model were used as initial guesses of the control variables. Using data assimilation to compute the optimal tidal forcing along the open boundary led to better results than using the tidal open boundary conditions from Schwiderski global model. In this case, RMS errors between the tidal predictions and model results with the

optimal open boundary conditions are generally less than 15 cm for all 21 tidal stations and less than 5 cm for the nine coast stations from which the data were used in assimilation. The correlation coefficients between tidal predictions and model results with the optimal open boundary conditions are greater than 0.96. Comparison between the results from the experiment PA_CTC, in which five tidal constituents were considered together, and from the experiment, PA_ITC, in which five tidal constituents were individually considered, showed that the optimal amplitude and phase of each of the five tidal constituents at the open boundary from the two experiments are not exactly same, but the optimal amplitudes and phases of the predominate M_2 constituent are very close. The optimal open boundary elevations obtained from the two experiments are therefore almost the same (the average difference for 30 day period is less than 0.1 cm), which, in turn, leads to the result that the RMS errors and correlation coefficients of these two experiments at the 21 tidal stations are very close. However, the experiment PA_CTC is much more efficient than PA_ITC.

In the present study, only open tidal boundary conditions were treated as control variables and tidal predicted elevations were assimilated. Thus, only the errors of the simulated elevations caused by inaccurate open boundary conditions were corrected. However, for total water level-simulations, there may be errors produced by other effects. For the purpose of a real-time water level nowcast/forecast, the accuracy of total water-level should be improved by adjusting surface wind forcing and other parameters.

Acknowledgements

We thank the anonymous reviewers from Continental Shelf Research for their valuable comments on the manuscript. Dr. Kurt Hess and Dr. Tom Gross are also appreciated for their constructive comments during the internal reviews. Aijun Zhang conducted this work while he is a UCAR visiting scientist in CSDL.

References

Bennett, A.F., 1985. Array design by inverse method. Progress in Oceanography 15, 129–156.

Bennett, A.F., McIntosh, P.C., 1982. Open ocean modeling as an inverse problem: tidal theory. Journal of Physical Oceanography 12, 1004–1018.

Blumberg, A.F., Mellor, G.L., 1987. A description of a three-dimensional coastal ocean circulation model. In: Heaper, N.S. (Ed.), Three Dimensional Coastal Ocean Models. American Geophysical Union, Washington, DC, pp. 1–16.

Cacuci, D.G., 1988. The forward and adjoint methods of sensitivity analysis. In: Ronen, Y. (Ed.), Uncertainty Analysis. CRC Press, Boca Raton, FL, 282pp.

Chen, P., Mellor, G., 1999. Determination of tidal boundary forcing using tide station data. In: Mooers, C.N.K. (Ed.), Coastal Ocean Prediction, Vol. 56, CRC Press, Boca Raton, FL, pp. 329–351.

Egbert, G.D., Bennett, A.F., Foreman, M.G.G., 1994. TOPEX/POSEIDON tides estimated using a global inverse model. Journal of Geophysical Research 99, C12, 24821–24852.

Hall, M.C.G., Cacuci, D.G., Schlesinger, M.E., 1982. Sensitivity analysis of a radiative-convective model by adjoint method. Journal of Atmospheric Science 39, 2038–2050.

Han, G., Fang, G., Ma, J., Liu, K., Li, D., 2000. Optimizing open boundary conditions of nonlinear tidal model. ACTA Oceanologica Sinica 22 (4), 1–7.

Heemink, A.W., Mouthaan, E.E.A., Roest, M.R.T., Vollebregt, E.A.H., Robaczewska, K.B., Verlaam, M., 2002. Inverse 3D shallow water flow modeling of the continental shelf. Continental Shelf Research 22, 465–484.

Lawson, L.M., Spitz, Y.H., Hofmann, E.E., Long, R.B., 1995. A data assimilation technique applied to a predator-prey model. Bulletin of Mathematical Biology 57, 593–617.

Liu, D., Nocedal, J., 1989. On the limited memory BFGS method for large scale optimization. Mathematical Programming B 45, 503–528.

Schwiderski, E.W., 1980. On charting global ocean tides. Reviews of Geophysics and Space Physics 18, 243–268.

Seiler, U., 1993. Estimation of open boundary conditions with the adjoint method. Journal of Geophysical Research 98, 22855–22870.

Zhang, A., Parker, B.B., Wei, E., 2002a. Assimilation of water level data into a coastal hydrodynamic model by an adjoint optimal technique. Continental Shelf Research 22, 1909–1934.

Zhang, A., Parker, B.B., Wei, E., 2002b. Development of an east coast water level data assimilation model. US Department of Commerce, NOAA Technical Report, OCS 13, 102pp.